AJNR

Distinguishing between scar and recurrent herniated disk in postoperative patients: value of contrast-enhanced CT and MR imaging.

C V Bundschuh, L Stein, J H Slusser, F P Schinco, L E Ladaga and J D Dillon

AJNR Am J Neuroradiol 1990, 11 (5) 949-958
http://www.ajnr.org/content/11/5/949

Distinguishing Between Scar and Recurrent Herniated Disk in Postoperative Patients: Value of Contrast-Enhanced CT and MR Imaging

Carl V. Bundschuh[1]
Lee Stein[2]
James H. Slusser[3]
Frank P. Schinco[4]
Leopoldo E. Ladaga[5]
James D. Dillon[4]

Twenty patients with failed back surgery syndrome were analyzed prospectively with MR imaging. In addition, 10 of these patients were analyzed with high-dose contrast-enhanced CT or gadopentetate dimeglumine–enhanced MR imaging. Imaging results were compared with surgical and pathologic findings in all cases. In the 10-patient subset, abnormal epidural soft-tissue specimens were also assessed with light and electron microscopy for vascular density, size of the extracellular space, and collagen orientation and thickness. The average vascular density of epidural fibrosis on light microscopy was found to be 1.19%; the average size of the extracellular space on electron microscopy was 4.29%. Scar 4 months of age or less had a larger extracellular space than did older scar; high- (grade 4 or 5) intensity scar had a larger extracellular space than did less intense scar on long TR/short TE images. Scar 1 year old or less enhanced more intensely on CT than did older scar. The MR signal intensity and CT enhancement characteristics of epidural scar were also found to differ according to epidural location. The percentage of scar that was hyperintense on long TR/TE images was as follows: anterior, 82%; lateral recess, 70%; lateral, 47%; and posterior, 20%. However, no relationship was found between the degree of CT enhancement of scar and vascular density.

Gap junction status and extracellular space size, therefore, are more important than vascular density in predicting the degree of enhancement. The accuracy of contrast-enhanced CT and unenhanced MR in separating scar from herniated nucleus pulposus is 80%. This accuracy is related to the partial overlap in imaging characteristics of scar and recurrent herniated nucleus pulposus.

AJNR **11:949–958, September/October 1990**

The severity of symptoms in the failed back surgery syndrome has not been shown to correlate with the amount of epidural scar tissue [1]. Furthermore, the presence of recurrent or residual herniated nucleus pulposus (HNP) generally is thought to be an indication for repeat surgical intervention [2–6]. However, although the mechanism for contrast enhancement of epidural scar and HNP has been suggested [2–7], to our knowledge no detailed histologic analysis with a moderate number of patients has been performed correlating enhancement and signal-intensity characteristics with vascular density, extracellular space size, and other variables. In addition, there is a wide variation in the reported ability of MR imaging or contrast-enhanced CT to accurately separate epidural fibrosis from HNP, as well as a lack of agreement about their imaging characteristics [1–7]. In an attempt to clarify these differences, we assessed scar by age and epidural location in a prospective imaging, surgical, and histologic analysis of abnormal epidural soft tissue in 20 patients (22 vertebral levels) with failed back surgery syndrome.

Subjects and Methods

Twenty patients (28–75 years old; average age, 46.4 years) with failed back surgery syndrome were enrolled in a prospective study to assess the accuracy of MR in the evaluation

Received September 7, 1989; revision requested November 13, 1989; final revision received April 17, 1990; accepted April 19, 1990.

[1] Department of Diagnostic Radiology, Sentara Norfolk General Hospital, 600 Gresham Dr., Norfolk, VA 23507. Address reprint requests to C. V. Bundschuh.

[2] Eastern Virginia Medical School, Lewis Hall, P.O. Box 1980, Norfolk, VA 23501.

[3] Department of Anatomy, Eastern Virginia Medical School, Lewis Hall, P.O. Box 1980, Norfolk, VA 23501.

[4] Department of Neurosurgery, Eastern Virginia Medical School, Hofheimer Hall, Room 201, 625 Fairfax Ave., Norfolk, VA 23507.

[5] Department of Pathology, Sentara Norfolk General Hospital, Norfolk, VA 23501.

0195-6108/90/1105-0949

of abnormal epidural soft tissue. Contrast-enhanced CT was performed in nine of the 20 patients and gadopentetate dimeglumine–(Berlex Labs., Cedar Knolls, NJ) enhanced MR was performed in one patient. All imaging results were compared with surgical and gross pathologic findings. After the dual examination, scar and HNP specimens from the 10-patient subset were sent for further investigation with light and transmission electron microscopy. For this group, the average time between the previous operation and imaging studies was 14.2 months (range, 2 months to 3.7 years). The sample range for the entire study population was 2 months to 16 years (average, 36.8 months). Informed consent and local Institutional Review Board approval were obtained for all patients. Patients who had previously experienced severe reactions to high-osmolality contrast material were excluded from the study.

A 1.5-T superconducting magnet (Signa, General Electric Medical Systems, Milwaukee) was used with a 55-cm body coil and a 14.0-cm circular, planar, receive-only surface coil. Sagittal 3-mm contiguous short TR/TE spin-echo images, 600–800/20–30/2 (TR/TE/excitations), were acquired with a 256 × 256 matrix and a 24-cm field of view. Axial long TR/short and long TE spin-echo images, 2000–2500/20–40, 80–120/2, were obtained with a 3-mm slice thickness, a 1.5-mm interslice gap, a 256 × 128 matrix, and a 24-cm field of view, displayed after computer magnification. These images were supplemented with an axial 3-mm short TR/TE sequence (600–800/20–30). In the one patient with gadopentetate dimeglumine enhancement, administered at a dose of 0.1 mmol/kg, repeat short TR/TE axial images were acquired within 10 min of contrast injection.

The details for the acquisition of the unenhanced and contrast-enhanced CT images are described elsewhere [3]. Briefly, a total of 300 ml of high- or low-osmolality contrast material were used. The patients received low-osmolality contrast material if they were older than 50, had a recent myocardial infarction or severe congestive heart failure, had a history of atopy or asthma, were diabetic, had a mild to moderate reaction to high-osmolality contrast material, or had evidence of preexisting renal disease. Contrast-enhanced CT was completed no later than 10 min after the initiation of IV delivery of contrast material.

MR was performed within an average of 12.5 days of the CT study. Tissue specimens were obtained within an average of 4.1 days from imaging for the subset of patients with detailed histologic analysis and within 20.1 days for the remainder.

Predictions concerning the nature of the abnormal epidural soft tissue were relayed to the surgeon prior to reoperation. One of us was also present at surgery to further aid in identification of abnormal soft tissue and to guide the collection of specimens defined by the MR or CT studies. Scar specimens were labeled by epidural location [2, 3], placed in normal saline, and transported within an hour to pathology, where they were separated and placed in their respective fixatives (10% buffered formalin or Karnovsky fixative). Several HNP specimens and one skeletal muscle biopsy, obtained from the paraspinous musculature, were treated in a similar fashion.

After a portion of the specimen was fixed in formalin and embedded conventionally in paraffin, it was stained with hematoxylin and eosin, Masson trichrome, and in most instances a reticulin stain. The sample was then photographed at ×4, ×40, and ×100 magnification. Although at least nine different portions of each specimen were examined, only one to three of the most vascular regions were photographed per sample. After a buffer rinse, the remainder of the sample was treated with 1% osmium tetroxide solution for 1–2 hr. It was then dehydrated through a graded series of ethanol concentrations and transferred to propylene oxide. With the use of Polybed 812 resin for infiltration and embedment, subsequent blocks were sectioned with a diamond knife, stained with uranyl acetate and lead citrate, and viewed on a Philips EM 301 transmission electron microscope. Seven to nine separate areas of each scar sample were photographed at a magnification of ×1900.

Light photomicrographs were then used for determinations of vascular density. Only vessels oriented at right angles to the plane of section were used for analysis. The electron photomicrographs were used for assessment of extracellular space. Although many of the cell bodies were disrupted during the hour the specimens remained in the operating room in a saline solution, on higher-power views all specimens used for data on extracellular space size (eight scar sites, 60 data points) showed collagen's normal periodicity, indicating adequate collagen preservation (Fig. 1). Because cell bodies were encountered infrequently, the cellular disruption was not considered significant. Therefore, we defined the electron-lucent and slightly electron-dense areas between collagen fibers and fibrils as extracellular space. Small areas between collagen fibrils were not included in the analysis. Both stereologic studies were performed with the use of an Optomax statistical image analysis computer system (Optomax, Division of ITI, Burlington, MA) in conjunction with a digitizer pad [8].

The electron photomicrographs were also assessed visually by one of us for collagen orientation and thickness. Grade 1 represented delicate, loosely arranged collagen fibrils; grade 3, thick and well-oriented collagen fibers. Signal intensity on T1-, spin-density-, and T2-weighted MR of abnormal epidural soft tissue was visually compared with the intensity of the cancellous portion of the adjacent vertebral body (upper or lower third). Relative intensity was graded on a scale of 1–5, with 1 representing marked hypo-, 3 representing iso-, and 5 representing marked hyperintensity. Contrast enhancement on CT was rated from 0 to 3, with 0 indicating no enhancement, 1 mild enhancement, 2 moderate enhancement, and 3 marked enhancement. Grade 3 enhancement was noted to be similar to the density of the prevertebral vasculature; that is, aorta, vena cava, and their pelvic branches. Post–gadopentetate dimeglumine enhancement on short TR/TE MR was graded 3 when similar to that of fat, at the same depth from the surface coil as the abnormal soft tissue.

Analysis of variance (Duncan's multiple range test for variable), Student's t test, Fisher's exact test, and chi square were used for statistical assessment of the data. Applications of these tests are described further in the Results section.

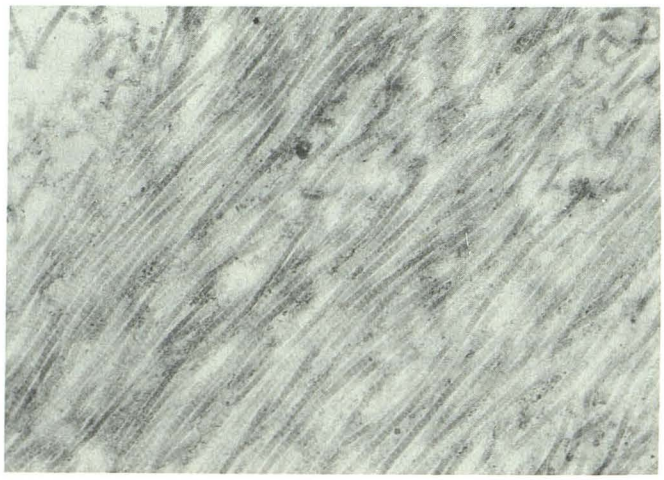

Fig. 1.—Case 10. Periodicity of collagen is seen, indicating good fixation and accurate depiction of its in vivo status. (Original magnification, ×15,000)

TABLE 1: Summary of CT Enhancement and T2-Weighted MR Intensity Characteristics in the Evaluation of Abnormal Epidural Soft Tissue

Case No.	Time Between Operation and Imaging	Epidural Scar								HNP		Operative/Histologic Findings
		Anterior		Lateral Recess		Lateral		Posterior		IVCT	T2WI	
		IVCT	T2WI	IVCT	T2WI	IVCT	T2WI	IVCT	T2WI			
1	2 mo	1	5	2	5	3	1	3	1	0	5	HNP (prolapse), epidural scar
2	3 mo	NS	NS	2	4	2	5	3	3	3	3	Focal bulge, epidural scar
3	3.5 mo	2	5	1	4	?	4	0	1	0 0	5[a] 4[b]	HNP (free), epidural scar
4	3.7 yr	NS	NS	1	5	1	5	1, 0	1, 1	0	3	Osteophyte, epidural scar
5	6 mo	2	3	2.5	3	2	3	2	3	0	3.5	HNP (free), epidural scar
6	11 mo	NS	NS	3	3	NS	NS	1	1	3 0	5[c] 2[d]	HNP (free & extruded), epidural scar
7	2 yr	2	3	1	5	NS	NS	0	1	2	3	HNP (free), epidural scar
8	3 mo	3	5	2.5	3	2.5	3	2	4	0	5	HNP (free), epidural scar
9	1.3 yr	1	5	1	5	1	3	0	3	0	3	HNP (extruded), epidural scar
10	6 mo	3	4	2	4	1	3	1	3	3	5	HNP (free), epidural scar
11	2 mo	NP	NS	NP	5	NP	NS	NP	5	NP	NS	Epidural scar
12	5 yr	NP	3	NP	3	NP	3	NP	2	NP NP	3.5[e] 3[f]	Large HNP (free), epidural scar; no disk protrusion
13	2 mo	NP	NS	NP	5	NP	3	NP	3	NP	5	HNP (free), epidural scar
14	6 yr	NP	NS	NP	NS	NP	NS	NP	NS	NP	4	HNP (free)
15	6 yr	NP	NS	NP	3	NP	NS	NP	3	NP	3	HNP (prolapse), epidural scar
16	5 yr	NP	NS	NP	3	NP	3	NP	3	NP NP	3[c] 4[d]	HNP (extruded & free), epidural scar
17	2 mo	NP	5	NP	3	NP	4	NP	5	NP	3[g]	Posterior anular bulge, epidural scar
18	7 yr	NP	NS	NP	4	NP	NS	NP	NS	NP	NS	Epidural scar
19	2 yr	NP	4	NP	4	NP	4	NP	3	NP	NS	Epidural scar, L5–S1
		NP	4	NP	4	NP	4	NP	4	NP	2[h]	Epidural scar, L4–L5
20	16 yr	NP	NS	NP	5	NP	2	NP	1	NP	NS	HNP, epidural scar

Note.—IV contrast-enhanced CT (IVCT) findings were graded on a scale of 0–3: 0 = no enhancement; 1 = mild enhancement; 2 = moderate enhancement; 3 = marked enhancement. T2-weighted MR imaging (T2WI) findings were rated on a scale of 1–5: 1 = marked hypointensity; 3 = isointensity; 5 = marked hyperintensity. HNP = herniated nucleus pulposus; ? = not seen owing to streak artifact; NP = not peformed; NS = not seen.

[a] Superior.
[b] At disk space.
[c] Extruded HNP.
[d] Free HNP.
[e] L3–L4.
[f] Focal bulge or prolapse, L4–L5.
[g] Posterior bulge.
[h] Central disk protrusion and osteophyte.

Results

Table 1 lists the enhancement and long TR/TE intensity characteristics of epidural fibrosis characterized by scar sites found in this study. Prospective determination of the presence or absence of HNP, its imaging characteristics, and operative/histologic findings are also noted.

Signal intensity of fibrosis, regardless of age, compared with epidural location is shown in Table 2. The frequency of moderate or marked hyperintensity (grade 4 or 5), noted on

long TR/TE images, was significantly greater than expected anteriorly and less than expected posteriorly (chi square, $p = .002$) (Fig. 2A). Lateral recess and lateral scar, as well as the intensity of every epidural site imaged with a short TR/TE or long TR/short TE spin-echo sequence, did not differ significantly from expected values. All anterior, lateral recess, and lateral scars enhanced after the administration of iodinated contrast material or gadopentetate dimeglumine (Figs. 2B and 2C). Four of 11 posterior scars did not enhance. The average CT enhancement grades were 2.0 for anterior, 1.8 for lateral recess, 1.8 for lateral, and 1.2 for posterior scar.

TABLE 2: Signal Intensities of Epidural Fibrosis in 20 Patients

Epidural Location	No. (%)			
	Hypo-, Isointensity, Short TR/TE	Hyperintensity		Total
		Long TR/ Short TE	Long TR/ Long TE	
Anterior	11 (100)	5 (45)	9 (82)	11
Lateral recess	19 (95)	6 (30)	14 (70)	20
Lateral	13 (87)	8 (53)	7 (47)	15
Posterior	18 (90)	4 (20)	4 (20)	20
Total	61 (92)	23 (35)	34 (52)	66

Note.—Signal intensity was assessed relative to the cancellous portion of the adjacent vertebral body.

By using analysis of variance, we found that scar 1 year of age or less enhanced significantly more than older scar ($p = .01$) (Figs. 3 and 4). Scar 4 months old or less had a mean extracellular space size on electron microscopy of 6.65%, which was significantly larger ($p = .001$) than the extracellular space size of 3.49% found in older scar (Fig. 5). When correlated with scar age, no significant differences were found in mass effect of anterior and lateral recess scar or in long TR/TE image intensity of epidural scar taken as an aggregate.

Grade 4 or 5 hyperintensity seen on long TR/short TE images indicated a larger extracellular space than less intense scar ($p = .0001$). Grade 5 hyperintensity denoted the same thing on a long TR/TE sequence; however, grade 1 intensity on a short TR/TE image indicated a significantly smaller extracellular space ($p = .0001$, analysis of variance).

The mean vascular density of epidural scar of all ages and scar sites was 1.19%. The mean vascular density of skeletal muscle, biopsied from the paraspinous musculature, was 0.69%. This indicates a trend, though no significant difference between these values was found by using Student's t test ($p = .08$). The mean extracellular space sizes of epidural scar and muscle were found to differ significantly ($p = .0001$); for scar the value was 4.29% and for muscle it was 0.79%. The

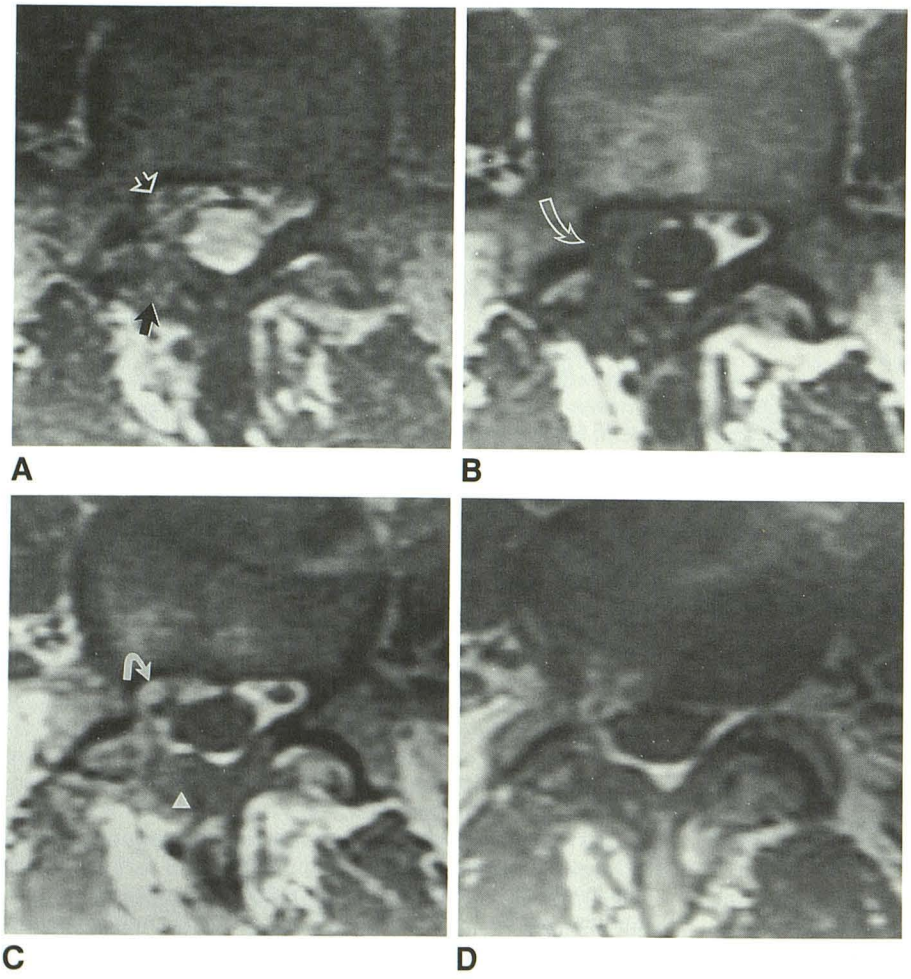

Fig. 2.—Case 10: 6-month scar and free herniated nucleus pulposus, L4–L5.

***A*, Long TR/TE image (2500/80). Punctate hypointensities seen anteriorly represent portions of anterior internal vertebral veins as well as right L5 ventral and dorsal nerve roots. Note grade 4 intensity in anterior epidural space and lateral recess (*open arrow*) and grade 3 intensity posteriorly (*solid arrow*).**

***B*, Short TR/TE image (600/20) shows mildly hypointense scar (grade 2) extending from right anterior epidural space to hemilaminectomy. Note partial facetectomy (*arrow*).**

***C*, Enhanced short TR/TE image (600/20) shows grade 3 enhancement anteriorly (*arrow*) and predominantly grade 1 enhancement of hemilaminectomy scar (*arrowhead*).**

***D*, Enhanced short TR/TE image (600/20) at L4–L5 interspace shows thick peripheral enhancement (grade 3) of free disk fragment anterolateral to posteriorly displaced right L5 nerve root sleeve.**

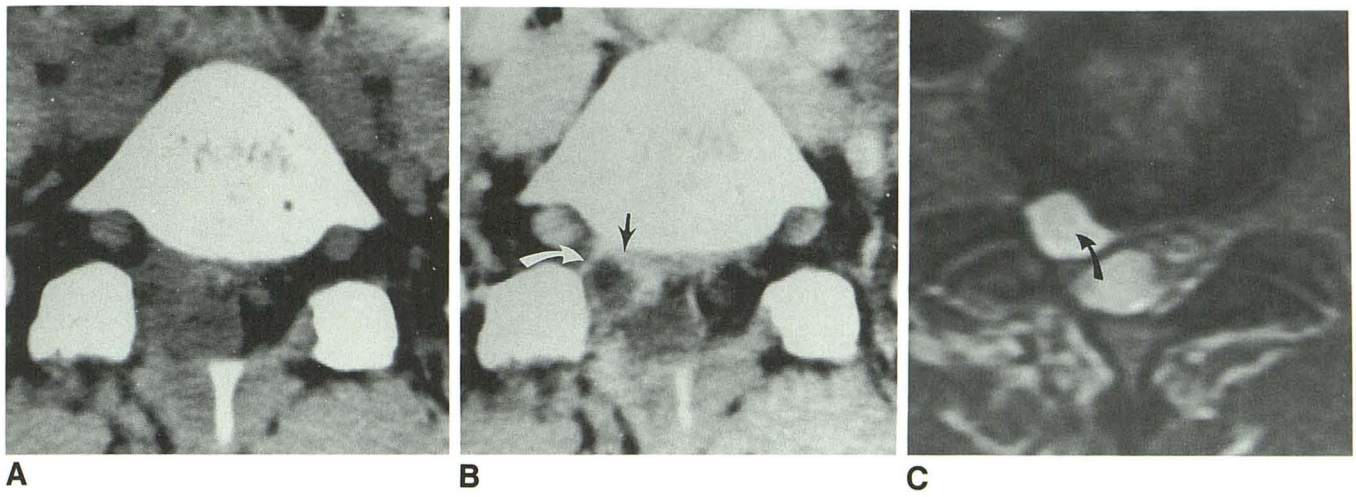

Fig. 3.—Case 8: 3-month scar. L5–S1.

***A* and *B*, Unenhanced (*A*) and bolus contrast-enhanced (*B*) nonangled CT images show grade 3 enhancement in anterior epidural space (*black arrow*) and grade 2–3 enhancement in lateral recess (*white arrow*). Dorsal nerve root ganglia also enhance. This can be a normal finding.**

***C*, Long TR/TE image (2500/80) parallel to L5–S1 disk shows markedly hyperintense anterior and lateral recess scar (grade 5), indistinguishable from adjacent free disk fragment (*arrow*).**

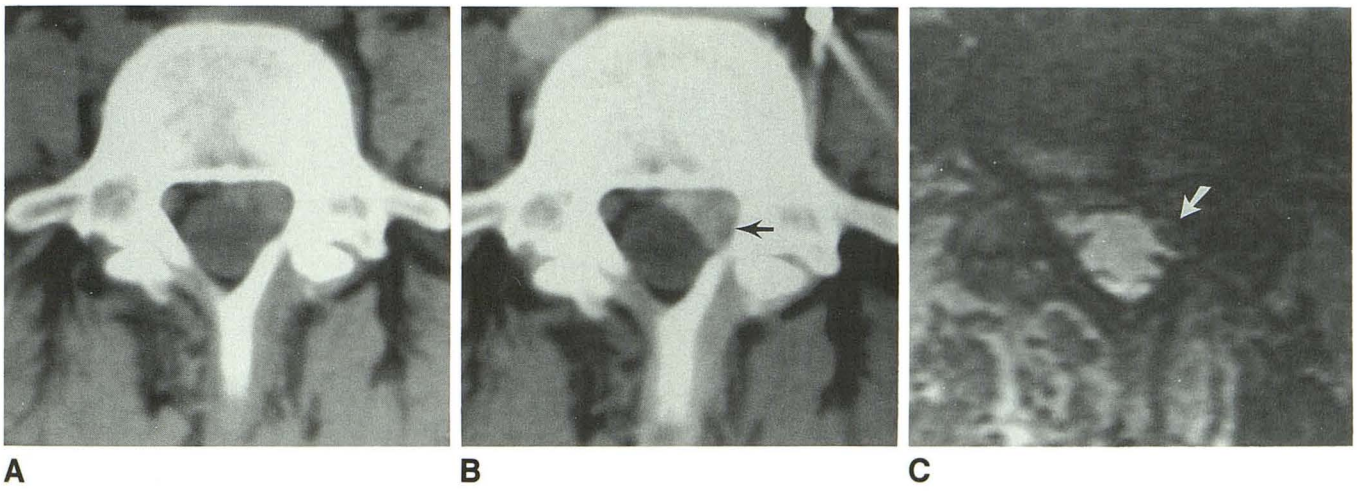

Fig. 4.—Case 5: 6-month-scar, L4–L5.

***A* and *B*, Unenhanced (*A*) and contrast-enhanced (*B*) CT images show a large anterior and lateral recess soft-tissue mass with heterogeneous grade 2–3 enhancement. Focal areas of nonenhancement laterally are in part related to left L5 nerve roots (*arrow*). Note mild mass effect on dural tube.**

***C*, Long TR/TE image (2500/80) reveals isointense (grade 3) anterolateral scar (*arrow*) with obvious mass effect on adjacent thecal sac. Only 30% of all lateral recess scars are hypo- to isointense on long TR/TE sequences.**

average vascular density of epidural scar did not correlate with its enhancement grade. The numbers in this group were too small to subdivide vascular density by scar site or age and compare with enhancement grade. Collagen orientation and thickness also did not correlate significantly with intensity on long TR/TE images.

Five of 10 previously operated intervertebral disks demonstrated generalized anular enhancement. One of two extruded HNPs (Fig. 6) and two of six free HNPs (Figs. 2D and 7) enhanced also. The enhancement was patchy and central in two and peripheral and thick in one (Fig. 2D). One focal bulge enhanced homogeneously. All focal bulges and prolapses were hypo- to isointense on long TR/TE sequences. Nine of 10 free HNPs were hyperintense on long TR/TE images; however, only one was hyperintense on a short TR/TE acquisition.

Table 3 indicates that of the four imaging characteristics of aberrant soft tissue in the anterior epidural space or lateral recess, three are important in the discrimination of scar from HNP ($p < .0001$, Fisher's exact test). Intensity is shown to be of little value, although half the herniations in Table 3 are free HNPs.

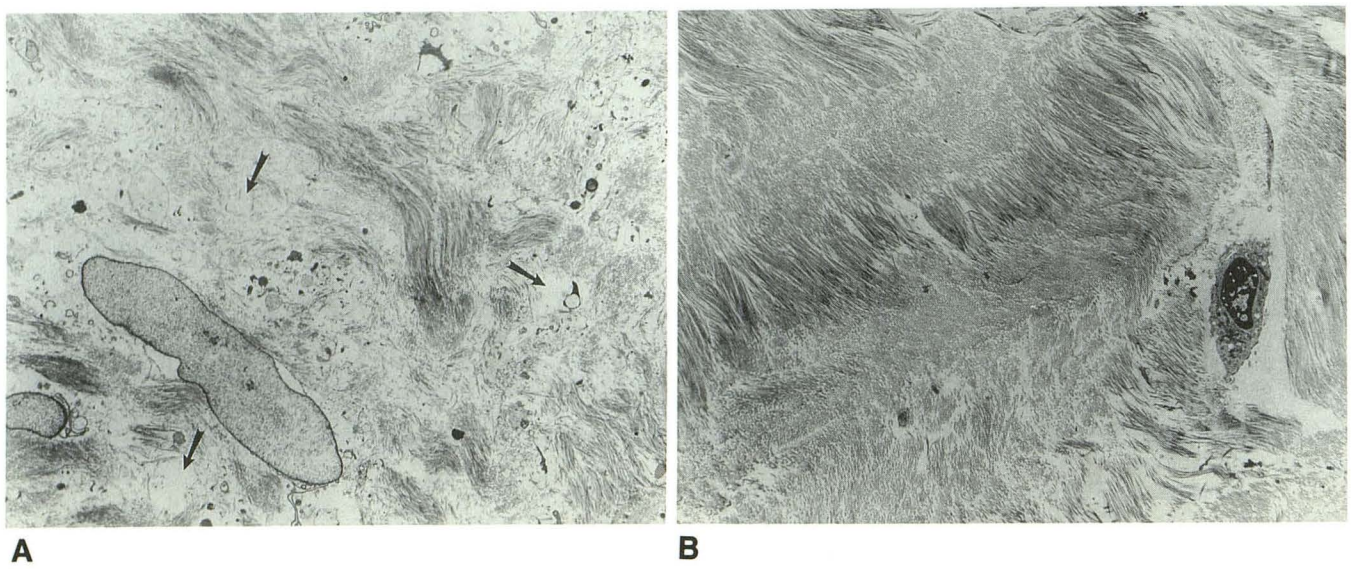

Fig. 5.—Transmission photomicrographs of scar specimens.
A, Case 2: 3-month immature scar. Note prominent extracellular space (*arrows*) and sparse deposition of collagen. Extracellular space comprises 7.9%. (Original magnification, × 1900)
B, Case 4: 3½-year mature scar. Compact collagen, with dramatic decrease in size of extracellular space. Extracellular space comprises 2.4%. (Original magnification, × 1900)

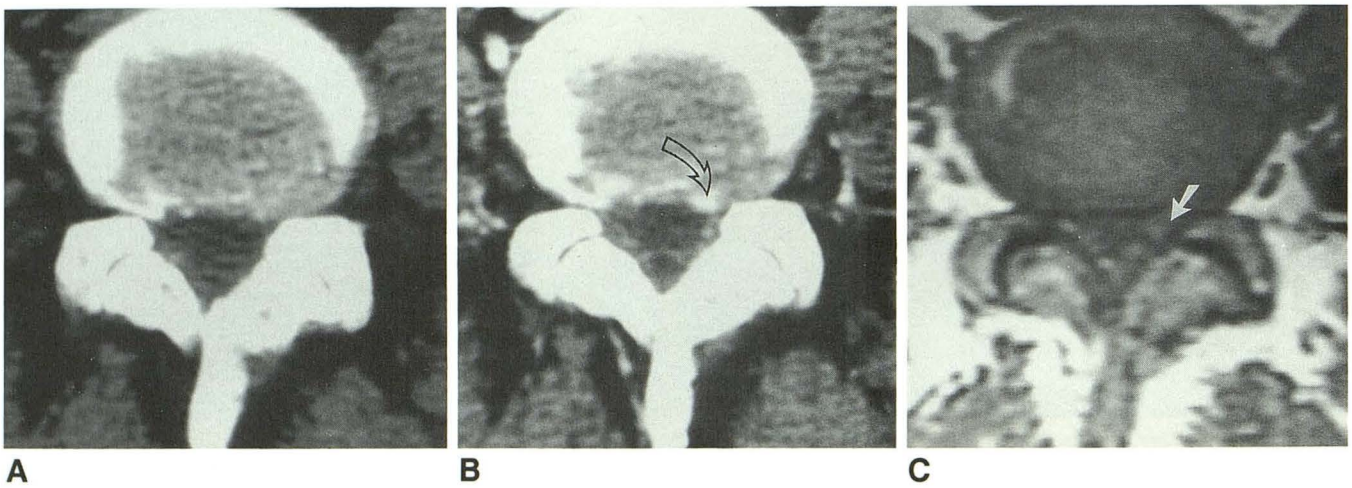

Fig. 6.—Case 6: Extruded herniated nucleus pulposus (HNP) and epidural scar; mild posterior anular bulge, L4–L5.
A and *B*, Unenhanced (*A*) and bolus contrast-enhanced (*B*) CT scans. Prominent central grade 3 enhancement (*arrow*) in extruded HNP. Epidural scar was seen better on other sections.
C, Short TR/TE image (800/20) shows triangular grade-3-intensity HNP in left lateral recess of L5 (*arrow*).

The prospective prediction with MR fully agreed with surgical and histologic findings at only 18 (81.8%) of 22 previously operated levels. The agreement fell to 70% with the use of contrast enhancement, because of the enhancement of three HNPs. If the percentage of levels where appropriate therapy was suggested is considered, the combination of unenhanced MR and a contrast-enhanced CT study led to an accuracy of 80%.

Discussion

Scar tissue is a metabolically active material that undergoes considerable change from inception to maturation. The changes, which can be seen in every constituent of scar, may be classified as either biochemical or morphologic.

Capillaries in granulation tissues have scanty micropinocytotic vesicles, an inconsistent orientation, a thick basal lamina, a high frequency of luminal occlusion or near occlusion [9, 10], a high density [11], only a loose network of pericytes [12], probably much leakier junctional complexes [13–15], and a higher ratio of chondroitin 4- and 6-sulfate to dermatan sulfate [14]. In contrast, the microvasculature in mature scar shows no luminal occlusion, a rich amount of micropinocytotic vesicles, a thin basal lamina [10], a decrease in density [11], and a complete or nearly complete layer of pericytes [12]. From one phase of tissue injury to another, a changing

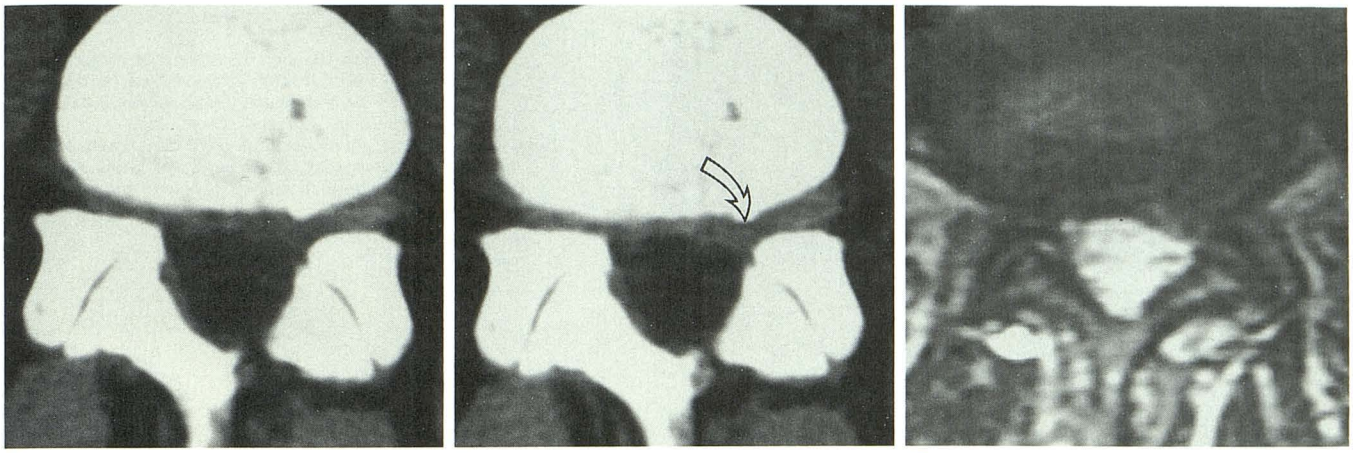

Fig. 7.—Case 7: Subligamentous free herniated nucleus pulposus (HNP) and epidural scar, L4–L5.
***A* and *B*, Unenhanced (*A*) and bolus contrast-enhanced (*B*) CT scans. Free HNP enhances centrally (*arrow*), along with peripheral enhancement secondary to scar and posterior longitudinal ligament.**
***C*, Long TR/TE (2500/80) sequence. Free HNP appears with grade 3 intensity. Mass effect is more obvious than on CT.**

TABLE 3: Imaging Characteristics of Anterior Epidural and Lateral Recess Soft-Tissue Masses

Variable	No. (%)	
	Scar	HNP
Within 4 mm of disk space	10 (32)	14 (88)
Greater than 4 mm from disk space	21 (68)	2 (12)
Mass effect[a]	9 (29)	16 (100)
Hyperintense (long TR/TE)	23 (74)	11 (69)
Enhancement[b]	17 (100)	3 (33)
Total	31	16

Note.—HNP = herniated nucleus pulposus.
[a] If questionable, considered positive.
[b] Scar in 17; HNP in nine.

metabolic state is reflected by these changes in the microvasculature, which may also occur at different rates.

Collagen also undergoes dramatic posttrauma changes with time. Within 1 week of injury, a fine meshwork of collagen fibrils restores tissue continuity. In a 3-week-old scar, fibrils are aggregating to form fibers—with the fiber orientation determined by location. In a 2½ to 4-month-old scar, collagen orientation has already changed to a mature status, but the fiber and fiber bundle is smaller than in a 1-year-old scar [16]. Immature nonhypertrophic scar demonstrates numerous fibroblasts and marked fibrillogenesis, though the amount of fibrosis present is strikingly less than in mature scar [11]. The water content of scar has been shown to change with scar age as well [17], with young scar containing more water than older scar.

The time over which these changes take place is variable, and depends on the type of injury and type and location of tissue involved. Mature scar resulting from tissue injury has been noted to form as early as 5 weeks after trauma, whereas hypertrophic scar can persist in an immature state for years [11].

Intervetebral disk changes with age, though on a much different time scale. In contrast to the weeks to months it commonly takes for scar tissue to mature, the degeneration of disk material occurs over a period of years. As a disk degenerates it dessicates, and through the cartilagenous endplates, Schmorl nodes, and anterior nuclear protrusions, vascular ingrowth can occur [18]. Herniated masses, consisting of nucleus pulposus with adherent lamellae of anulus, also show evidence of vascularization [19, 20]. The boundary between disk tissue and granulation tissue is usually sharp, although exceptions certainly exist (Fig. 8B). Scar tissue closer to an HNP is "looser" and more voluminous than the shrunken and more condensed distal scar [19]. Granulation tissue has been shown in 33–48% of herniated disk biopsy specimens [19, 20].

The morphology of tight junctions can be subdivided on the basis of the presence and frequency of fusion points between the outer leaflets of adjoining endothelial cells. Tight junctions normally allow molecules no larger than 2–3 nm to pass freely into the extravascular (extracellular) space [18]. Pinocytotic vesicles range from 60 to 100 nm in diameter [15], and the occasional large channels found in the discontinuous endothelium of human granulation tissue are about 20 nm wide [12]. As a frame of reference, albumin is 4.2 nm and has a molecular weight of 59,000; gadopentetate dimeglumine has a molecular weight of 938, iohexol (Winthrop Pharmaceuticals, New York, NY) of 821, iopamidol (Squibb Diagnostics, Princeton, NJ) of 777, and diatrizoate of 614. Therefore, at least loose tight junctions, pinocytotic vesicles, and larger inter- or transendothelial openings are potential paths for delivery of contrast material to the extracellular space.

The degree of contrast enhancement in a given tissue reflects the total amount of contrast material per unit volume and not necessarily just its vascularity. Local tissue contrast levels are, in part, affected by the size of the extracellular space and rates of diffusion between fluid compartments [17, 21]. Diffusion, in turn, is affected by the blood perfusion rate (which is proportional to lumen patency, vascular density, and cardiac output), the permeability of the capillary endothelium,

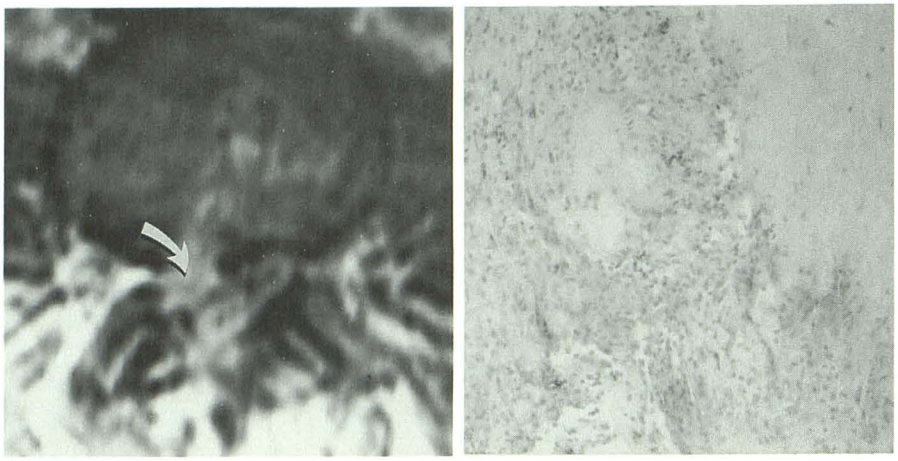

Fig. 8.—Case 12: 5 years from previous surgery, L3–L4.

***A*, Long TR/short TE (2500/40) image shows grade 4 right anterior epidural mass (*arrow*) with mass effect compatible with severely extruded or free disk fragment.**

***B*, Light photomicrograph. Hyperintense mass demonstrates fibrocartilage with granulation tissue embedded within. (Original magnification, ×40)**

and the initial vascular concentration of the contrast agent [21]. The blood perfusion rate is probably less in granulation tissue in comparison with mature scar, because of the higher rate of luminal occlusion or near occlusion. This also applies to hypertrophic scar. Furthermore, young scar most likely has leaky junctional complexes, and by many different criteria—including basement membrane thickness [22]—differs in permeability relative to old scar.

The effect of vascular density on contrast enhancement is modified by the above factors. Therefore, theoretically there may be no significant relationship between vascular density and contrast enhancement in a given tissue; experimentally we demonstrated this to be true for epidural fibrosis. We conclude that the size of the extracellular space and the status of the gap junction are the important determinants of contrast enhancement grade in scar [7, 23].

The relaxation rate, 1/T1, generally demonstrates a linear relationship to the percentage of water in a given volume of tissue. However, in tissues with equal proportions of water, 1/T1 may still differ. These differences can be related to the effects of macromolecular proteins, caused by the presence of bound and perhaps structured (hydration layer) water [24, 25]. Through the effects of cross relaxation via spin exchange [26]—and an increase in the correlation time [27], the spin-lattice relaxation time of the bound water fraction is shorter than that of the bulk fraction. The hydration layer, which is approximately three water layers, contributes to T2 shortening via motional restrictions. Indeed, given the anisotropy of the molecular motion of water on globular proteins [27] compounded with a somewhat uniform orientation, collagen fibrils, fibers, and fiber bundles should be associated with progressively lower signal intensities on long TR/TE images [28]. The long TR/short TE images in this series, reflecting predominantly proton-density contributions, correlated best with extracellular space size. In part this was because our short TR/TE sequences were not strongly, nor solely, T1-weighted. In fact, a T2 effect was noted on these sequences.

The significant association of only grade 5 hyperintensity on long TR/TE images with a large extracellular space is also probably related to a hydration layer effect. Although grade 4 or 5 hyperintensity on long TR/short TE images indicated a larger extracellular space than did less intense scar, and scar of 4-months duration or less had a significantly larger extracellular space than did older scar, the scar intensity on long TR images, taken as an aggregate, did not correlate with scar age. The reason for this discrepancy is twofold. One, for technical reasons, examination of scar specimens for the size of the extracellular space could be performed only for eight scar sites. Six of the eight sites were from the lateral or posterior epidural space; only one was from the anterior epidural space. Therefore, the determination of change in the size of the extracellular space with age was focused on a more quiescent scar site, where scar probably matures much more rapidly [17]. In fact, none of 11 posterior scar specimens were hyperintense on long TR sequences after 4 months, while three of seven young posterior scar specimens were hyperintense. This trend was not found anteriorly. Also, even though collagen orientation and thickness did not significantly correlate with scar intensity, we were unable to ascertain the in vivo fiber orientation. When correlating intensity directly to age, this may have had enough of an effect on scar intensity to change the level of significance. Other factors, such as the degree of cellularity and total macromolecular content, also may contribute to the intensity of epidural scar.

Scar is known to grow from the erector spinae muscles anteriorly [29]. Anterior scar could, on this basis alone, be in a slightly different stage of development. Because of the continual reparative processes occurring anteriorly, anterior epidural scar is probably younger, has a larger extracellular space, and is more heterogeneous than posterior scar [17]. It is also known that collagen fiber orientation differs by location in scar [16]. The mechanical stresses, which may be relayed to fibroblasts via piezoelectric forces [16], could be different in the anterior epidural space in comparison with the laminectomy site, thereby evoking differences in fiber orientation. These facts largely explain the long TR/TE signal intensity differences of anterior and posterior epidural scar noted in this study.

Free disk fragments have been reported to occasionally appear hyperintense on short TR/TE images [3]. This was found in only one of 10 sequestered HNPs. Disk material, like neurofibromas, is said to have a capacious extracellular space

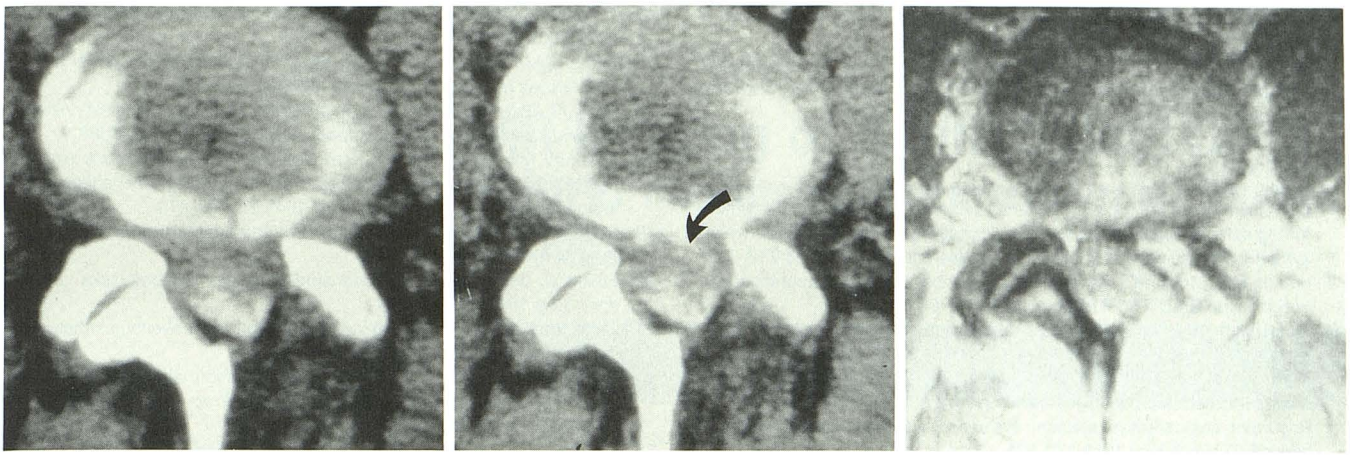

Fig. 9.—Severely extruded herniated nucleus pulposus (HNP) and epidural scar, L4–L5 (patient not in this study).
***A* and *B*, Unenhanced (*A*) and bolus contrast-enhanced (*B*) CT scans show grade 2–3 patchy central enhancement in a large extruded HNP (*arrow*).**
***C*, Long TR/short TE image (2000/30). Margins of HNP are defined better.**

[2, 28]. The mucopolysaccharide-rich myxoid matrix, thought to account for the intermediate signal intensity of these tumors on short TR/TE images, may account also for the relative hyperintensity of free HNPs.

The large extracellular space of disk material may also explain the early enhancement of three of nine HNPs in our study. Although the vascular granulation tissue was not homogeneously distributed throughout the HNP, the presence of vessels in the herniated specimen could certainly lead to early enhancement (Fig. 8B). This finding was noted by other investigators [6], and is at variance with the findings reported by Heuftle et al. [2]. Since CT has been reported to be less sensitive than MR for detecting contrast enhancement [30], and we have found an HNP in an unoperated patient that enhanced homogeneously and intensely on MR within 10 min of contrast administration, we believe that the early contrast enhancement of HNPs on CT (Figs. 6, 7, and 9) is most likely true for gadopentetate dimeglumine–enhanced MR also. More research in this area is required.

Muscle, as demonstrated by Ross et al. [7], enhances consistently less than does epidural scar. Our study showed that the extracellular space is smaller in muscle. Striated muscle has low, continuous endothelium, which implies tight junctional complexes. The microvasculature of granulation tissue in the retina has been demonstrated to be fenestrated with leaky intercellular junctions [15]. The vascular permeability of mature scar is most likely much different from that of granulation tissue. Therefore, the leakiness of scar's vasculature may or may not differ from muscle's vascular permeability, depending on scar age.

This study could be criticized on several grounds. First, we did not use an electronic cursor to measure Hounsfield units or signal intensity. Because of scar's heterogeneous enhancement on CT (making cursor placement critical) and noise caused by obesity or inclusion of streak or beam-hardening artifacts, quantitative measurements obtained electronically may lead to considerable intraobserver variation [31]. In addition, another study [32] has suggested that electronically obtained numeric intensity values offer no greater accuracy than does visual assessment. Further, we have found that strikingly different regions of intensity, assessed visually, may not differ dramatically when a cursor is used. Therefore, we believe that electronic measurements may be no more accurate than those done visually.

Our estimates of extracellular space size and vascular density are probably lower than values determined by other methods. However, if one assumes a hematocrit of 45%, the ratio of interstitial to plasma water volume of scar in our study averages 6.55. In dogs, it is 6.8 when using iothalamate [21]. The ratios are most likely close because of the systematic errors in our determination of vascular density and extracellular space size: only vessels at right angles to the section were counted, and small extracellular regions between collagen fibrils were ignored. These systematic errors appear to have canceled each other.

Conclusions

Gap junction status and extracellular space size are the dominant determinants of CT contrast enhancement in epidural scar, with vascular density playing a less important role. A large extracellular space correlates significantly with hyperintensity on long TR/short TE images because of the bulk water present, modified by the hydration layer, on long TR/TE sequences. Young scar enhances more intensely, and most likely has leaky junctional complexes. Collagen orientation and thickness appear to play a minor role in the long TR signal intensity of scar older than 2 months. In the clinical assessment, mass effect, location relative to the disk space, and enhancement characteristics help to separate scar from recurrent disk material. Intensity values used alone can lead to erroneous conclusions. Because of the overlap in imaging characteristics of scar and recurrent HNP, the predictive value of contrast-enhanced CT in conjunction with MR for accurately suggesting repeat operative intervention is 80%.

ACKNOWLEDGMENTS

We thank Barbara Joan Goldman for assistance in manuscript preparation and the technical staff working in CT and MR at Sentara Norfolk General Hospital for acquisition of the images.

REFERENCES

1. Cervellini P, Curri D, Volpin L, Bernardi L, Pinna V, Benedetti A. Computed tomography of epidural fibrosis after discectomy: a comparison between symptomatic and asymptomatic patients. *Neurosurgery* **1988**;23:710–713
2. Heuftle MG, Modic MT, Ross JS, et al. Lumbar spine: postoperative MR imaging with Gd-DTPA. *Radiology* **1988**;167:817–824
3. Bundschuh CV, Modic MT, Ross JS, Masaryk TJ, Bohlman H. Epidural fibrosis and recurrent disk herniation in the lumbar spine: MR imaging assessment. *AJNR* **1988**;9:169–178, *AJR* **1988**;150:923–932
4. Frocrain L, Duvauferrier R, Husson J-L, Noel J, Ramee A, Pawlotsky Y. Recurrent postoperative sciatica: evaluation with MR imaging and enhanced CT. *Radiology* **1989**;170:531–533
5. Sotiropoulos S, Chafetz NI, Lang P, et al. Differentiation between postoperative scar and recurrent disk herniation: prospective comparison of MR, CT, and contrast-enhanced CT. *AJNR* **1989**;10:639–643
6. Firooznia H, Kricheff II, Rafii M, Golimbu C. Lumbar spine after surgery: examination with intravenous contrast-enhanced CT. *Radiology* **1987**; 163:221–226
7. Ross JS, Delamarter R, Heuftle MG, et al. Gadolinium-DTPA–enhanced MR imaging of the postoperative lumbar spine: time course and mechanism of enhancement. *AJNR* **1989**;10:37–46, *AJR* **1989**;152:825–834
8. Parisien MV, McMahon D, Pushparaj N, Dempster DW. Trabecular architecture in iliac crest bone biopsies: infra-individual variability in structural parameters and changes with age. *Bone* **1988**;9:289–295
9. Kischer CW, Thies AC, Chvapil M. Perivascular myofibroblasts and microvascular occlusion in hypertrophic scars and keloids. *Hum Pathol* **1982**;13:819–824
10. Kirscher WC, Shetlar MR. Microvasculature in hypertrophic scars and the effects of pressure. *J Trauma* **1979**;19:757–764
11. Linares HA, Kischer CW, Dobrkovsky M, Larson DL. The histiotypic organization of the hypertrophic scar in humans. *J Invest Dermatol* **1972**;59:323–330
12. Weber K, Braun-Falco O. Ultrastructure of blood vessels in human granulation tissue. *Arch Dermatol Res* **1973**;248:29–44
13. Kischer CW. Fine structure of granulation tissues from deep injury. *J Invest Dermatol* **1979**;72:147–152
14. Donoff BR, Burke JF. Abnormality of hypertrophic scar blood vessels. *J Surg Res* **1978**;25:251–255
15. Tripathi RC, Tripathi BJ. Functional ultrastructure of endothelium. *Bibl Anat* **1977**;16:307–312
16. Hunter JAA, Finlay JB. Scanning electron microscopy of normal human scar tissues and keloids. *Br J Surg* **1976**;63:826–830
17. Ross JS, Blaser S, Masaryk TJ, et al. Gd-DTPA enhancement of posterior epidural scar: an experimental model. *AJNR* **1989**;10:1083–1088
18. Coventry MB, Ghormley RK, Kernohan JW. The intervertebral disc: its microscopic anatomy and pathology. Part III: pathological changes in the intervertebral disk. *J Bone Joint Surg* **1945**;27:460–474
19. Lindblom K, Hultqvist G. Absorption of protruded disk tissue. *J Bone Joint Surg* [*Am*] **1950**;32-A:557–560
20. Eckert C, Decker A. Pathological studies of intervertebral disks. *J Bone Joint Surg* **1947**;29:447–454
21. Newhouse JH. Fluid compartment distribution of intravenous iothalamate in the dog. *Invest Radiol* **1977**;12:364–367
22. Milici AJ, Furie MB, Carley WW. The formation of fenestrations and channels by capillary endothelium in vitro. *Proc Natl Acad Sci USA* **1985**;82:6181–6185
23. Kormano M, Dean PB. Extravascular contrast material: the major component of contrast enhancement. *Radiology* **1976**;121:379–382
24. Fullerton GD. Physiologic basis of magnetic relaxation: In: Stark DD, Bradley WG, eds. *Magnetic resonance imaging*. St. Louis: Mosby, **1988**:36–55
25. Bakker CJG, Vriend J. Multi-exponential water proton spin-lattice relaxation in biological tissues and its implications for quantitative NMR imaging. *Phys Med Biol* **1984**;29:509–518
26. Edzes HT, Samulski ET. The measurement of cross-relaxation effects in proton NMR spin-lattice relaxation of water in biological systems: hydrated collagen and muscle. *J Magn Reson* **1978**;31:207–229
27. Alvarez-Morugo AJ, Alvarez-Morugo A. New capillary collagen of cutaneous scans. *Acta Anat* (Basel) **1978**;102:385–391
28. Mitchell DG, Burk DL Jr, Vinitski S, Rifkin MD. The biophysical basis of tissue contrast in extracranial MR imaging. *AJR* **1987**;149:831–837
29. LaRocca H, Macnab I. The laminectomy membrane. Studies in its evolution, characteristics, effects and prophylaxis in dogs. *J Bone Joint Surg* [*Br*] **1974**;56-B:545–550
30. Nguyen CM, Ho K-C, Yu S, Haughton VM, Strandt JA. An experimental model to study contrast enhancement in MR imaging of the intervertebral disk. *AJNR* **1989**;10:811–814
31. Wilmink JT, Roukema JG. Effects of IV contrast administration on intraspinal and paraspinal tissues: a CT study. Measurement of CT attenuation numbers. *AJNR* **1987**;8:703–709
32. Sundaram M, McGuire MH, Schajowicz F. Soft-tissue masses: histologic basis of decreased signal (short T2) on T2-weighted MR images. *AJR* **1987**;148:1247–1250